Runaway Transition in Irreversible Polymer Condensation with Cyclisation

Maria Panoukidou,[1, *] Simon Weir,[1, *] Valerio Sorichetti,[2] Yair
Gutierrez Fosado,[1] Martin Lenz,[2, 3] and Davide Michieletto[1, 4, †]

[1]*School of Physics and Astronomy, University of Edinburgh,*
Peter Guthrie Tait Road, Edinburgh, EH9 3FD, UK
[2]*Laboratoire de Physique Théorique et Modèles Statistiques (LPTMS),*
CNRS, Université Paris-Saclay, F-91405 Orsay, France
[3]*PMMH, CNRS, ESPCI Paris, PSL University, Sorbonne Université, Université de Paris, F-75005, Paris, France*
[4]*MRC Human Genetics Unit, Institute of Genetics and Cancer,*
University of Edinburgh, Edinburgh EH4 2XU, UK

The process of polymer condensation, i.e. the formation of bonds between reactive end-groups, is ubiquitous in both industry and biology. Here we study generic systems undergoing polymer condensation in competition with cyclisation. Using a generalised Smoluchowski theory, molecular dynamics simulations and experiments using DNA and T4 ligase, we find that this system displays a transition, from a regime with finite-length chains at infinite time and dominated by rings to one dominated by linear polymers that grow in time. Finally, we show that fluids prepared close to the transition may have profoundly different compositions and rheology at large condensation times.

Linear polymer condensation is the process by which two polymeric end groups react and form a bond. It is one of the most common industrial processes to create long linear polymers [1], and is also relevant to DNA repair [2]. Classic theory of linear polymer condensation assumes that, in absence of loop formation, the average length of the reacting polymers diverges as $\langle l \rangle = 1/(1-p)$ where p is the extent of reaction [1, 3]. However, loop formation is expected to be favourable in certain conditions [4–7], yet difficult to precisely control during the synthesis [8]. The formation of loops in polymer condensation poses open challenges to both the theoretical and experimental polymer communities and significant efforts were made to understand the ring-chain equilibrium in reversible systems [7–12]. During irreversible polymer condensation, the formation of loops is expected to have a two-fold impact: structurally, it reduces the amount of reactable substrate that can form longer chains and, physically, it affects the rheological properties of the fluid [13]. Indeed, ring polymers are among the least understood classes of polymer architecture and have non-trivial static [14, 15] and rheological signatures [13, 16–20]. Due to the importance of chain topology in both dilute [21] and dense [13, 18, 19, 22–27] polymer solutions, it is thus important to understand the assembly kinetics of ring and linear polymer topologies during polymer condensation.

Here we study irreversible linear polymer condensation using a combination of theory, simulations, and experiments. First, we find that the competition of polymer condensation and cyclisation can be well described by a modified form of the Smoluchowski coagulation equation [28] with a sink term that captures the formation of loops. By spanning a broad range of polymer concentrations c, we discover that there is a runaway transition characterised by the fact that linear chains grow quickly enough to permanently escape cyclisation. This transition separates a regime in which all the polymers are converted into rings at infinite time (and hence do not grow with the extent of reaction), from one in which the mass fraction of ring polymers is finite, and the length of the linear chains diverges in time. Importantly, and in contrast to typical textbook pictures, this transition occurs at a finite, non-zero looping probability.

Finally, we show that as a consequence of this transition, systems prepared at similar initial concentrations close to the runaway transition and undergoing irreversible condensation will display markedly different architectural and rheological features at large enough condensation times. We conclude our paper by discussing the implications of our findings in the design of soft materials and molecular cloning.

Results – We first simulate linear condensation by means of Molecular Dynamics. We use a bead-spring polymer model [29] to simulate $l_0 = 174$ beads-long chains (bead size σ) diffusing in a box with periodic boundary conditions at monomer concentration c (see SI for details). The condensation process is modelled by creating an irreversible bond between two end-beads that are closer than 1.1σ in 3D space. The condensation is stochastic and occurs every $10^3 \tau_B$ ($\tau_B = \gamma\sigma^2/k_BT$ is the Brownian time and γ the friction) with probability $p_L = 0.1$ (Fig. 1a,b). During the simulation, we take snapshots of the system and record the list of bonds to reconstruct length and topology of the polymers (Fig. 1c). Over the simulation time, the number of initial linear chains decreases due to the formation of (i) longer linear polymers or (ii) circular chains (Fig. 1d). Additionally, lower monomer concentrations c promote the formation of more rings at large times and a slower decrease of the linear species. We also note that (i) the number frac-
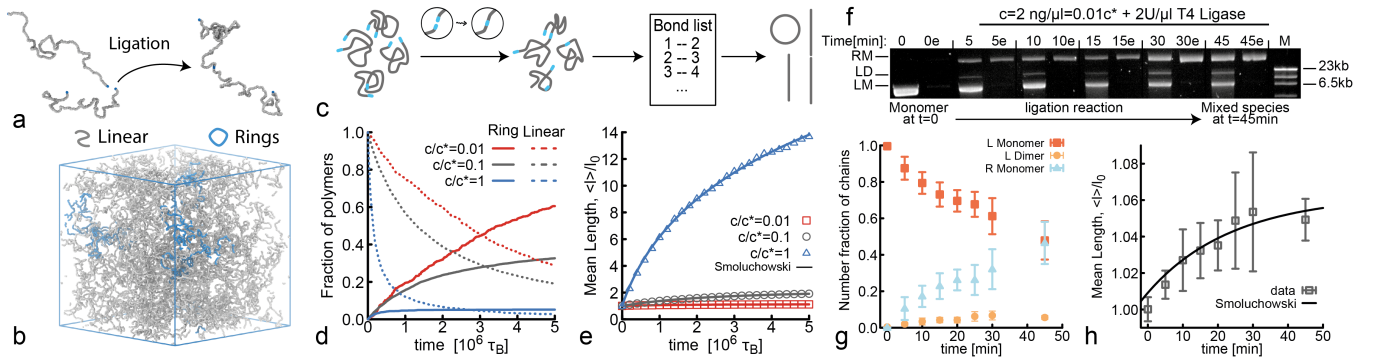
FIG. 1.   **a.** Molecular Dynamics simulations of polymer condensation. **b.** Snapshot of the simulation box with rings colored in blue and linear chains in grey. **c.** Pictorial representation of the simulation workflow, tracking the bond list to reconstruct length and topology of condensed polymers. **d.** Number fraction of linear and ring polymers during the condensation process for different choices of concentration c (averaged across 40 independent replicas). Note that the fraction of rings converge to a finite number at large time. **e.** Number averaged polymer length for the simulations in **d** as a function of time, and fitted with Eq. (1). **f.** Time-resolved gel electrophoresis during ligation of a 2 ng/ul ($c/c^* = 0.01$) solution of 6.5 kb linearised plasmid. The lanes marked with 'e' are treated with exonuclease to remove linear DNA; 'RM' indicates ring monomers, 'LD' linear dimers and 'LM' linear monomers. The last column is λ-HindIII marker to give a reference of DNA fragment lengths. The numbers at the top represent the minutes of ligation treatment. **g.** Number fraction of polymers in ring and linear (monomer and dimer) topologies. **h.** Number averaged length calculated from 3 independent gels at 2 ng/μl and associated fit using Eq. (1).

tion of rings converges to a finite value at large time, and that (ii) while the number of linear chains appears to go to zero, their length increases (as shown in detail below). Accordingly, the (number) average length of polymers, i.e. $\langle l \rangle = l_0 \sum_i n_i i / \sum_i n_i$, grows more quickly for larger c (Fig. 1e). Thus, we conclude that loop formation competes with the growth of the chains, and that cyclisation is dominant in dilute systems.

To validate our simulations we perform irreversible condensation on linear DNA using T4 ligase (NEB). This is an enzyme that consumes ATP to form a covalent bond between two proximal and complementary double-stranded DNA ends. More specifically, we perform irreversible condensation (also referred to as ligation henceforth) on a monodisperse solution of linear, $l_0 = 6.5$ kb-long, DNA at low concentrations $c = 2$ ng/μl $\simeq 0.01c^*$ ($c^* = 3l_0 M_w/(4N_A \pi R_g^3) \simeq 0.2$ μg/μl is the overlap concentration, $M_w = 650$ g/mol the molecular weight of a DNA basepair and N_A the Avogadro number). After adding T4 ligase, we draw aliquots at time intervals and heat-inactivate the reaction by heating the aliquot at $65°$C for 5 minutes. We then split the aliquot and treat one of the two sub-aliquots using exonuclease (RecBCD, Lucigen), an enzyme that digests linear, but not circular, DNA. Finally, we treat all aliquots with nickase, to relax torsional stress and remove supercoiling from the looped DNA [30]. By running the aliquots on agarose gels we can visualise and compute the fraction of molecules in the linear and ring, monomeric, dimeric, etc. states. Fig. 1f reports a picture of one such gel, showing a single band of monomeric linear DNA (as it disappears after exonuclease treatment) at $t = 0$, evolving into three bands, one of which is exonuclease resistant (a monomer ring) at larger times. In Fig. 1g we plot the relative abundance of these populations, from which we obtain the number average molecular length $\langle l(t) \rangle$ (Fig. 1h), which plateaus towards

a finite value at large ligation times.

To understand these measurements we propose a modified Smoluchowski coagulation equation:

$$\frac{dn_l}{dt} = \frac{1}{2} \sum_{i+j=l} k_1(i,j)n_i n_j - \sum_i k_1(i,l)n_i n_l - k_0(l)n_l \quad (1)$$

where n_l is the number density of chains of length l. The first two terms describe polymer condensation while the latter captures cyclisation. The rate of condensation k_1 is assumed to take the form [31, 32]

$$k_1(i,j) = \kappa_1 \left(i^{-\alpha} + j^{-\alpha} \right) (i^\nu + j^\nu) \sim (D_i + D_j)(R_i + R_j) \quad (2)$$

where D_i and R_i are the diffusion coefficients and size of polymer of length il_0, with α the dynamics exponent describing the dynamics and ν the metric exponent capturing the length-dependence of their size. The cyclisation rate is taken to be $k_0(l) = \kappa_0 l^\mu$, where $\mu = -4\nu$. Note that this is different from the classic Shimada-Yamakawa theory [33, 34] which would predict $\mu = -3\nu$ at $l \gg l_p$ (l_p the persistence length) because we (i) are out-of-equilibrium and (ii) account for the subdiffusion of the polymer end within the volume of the coil (see SI). Since we initialise our simulations and experiments below entanglement conditions, we fix $\alpha = 1$ as expected for Rouse dynamics and $\nu = 0.588$ as expected for self-avoiding polymers [35]. We numerically solve Eq. (1) and fit the data of mean length versus time, $\langle l(t) \rangle$, obtained in simulations and experiments via the free parameters κ_1 and κ_0 (Figs. 1e,h).

The key parameter in our system is the ratio of the rates at which linear polymers and rings are generated. We thus define a dimensionless "cyclisation parameter" $\kappa \equiv 2\kappa_0/(n_0\kappa_1)$, where n_0 is the number density of monomeric chains of length l_0 at the start of the simulation or experiment. Albeit related to the classic j-factor
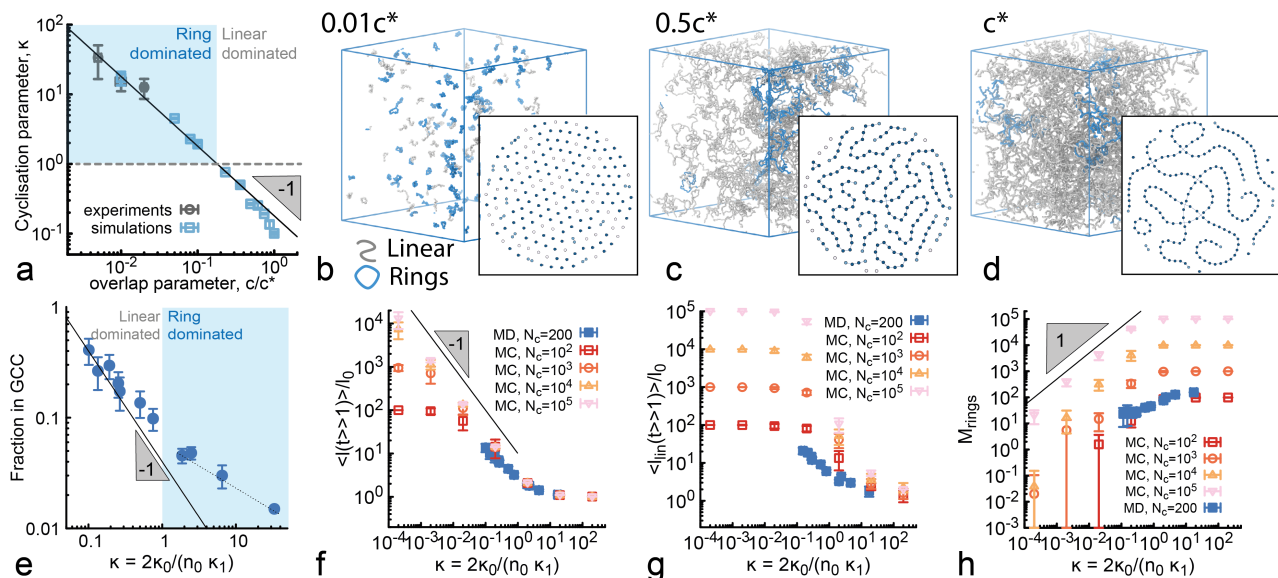
FIG. 2. **Runaway transition. a.** Dimensionless cyclisation parameter $\kappa = 2\kappa_0/(n_0\kappa_1)$ as a function of c/c^*. The scaling $\kappa \sim (c/c^*)^{-1}$ is consistent with κ_0 and κ_1 being independent on concentration and with this assumption breaking down near $c/c^* \simeq 1$. **b-d.** Snapshots of MD simulations with $N_c = 200$ monomers: the blue polymers represent rings of any length, grey polymers linear chains. In the network representations each circle i represents a monomer and its colour represents the number of chains connected to i: 0 (grey), 1 (cyan), or 2 (blue). A linear monomer is grey, a ring monomer blue, a linear dimer has two cyan nodes, and a dimer ring would have two blue nodes. **e** Fraction of monomers in the giant connected component as a function of κ. **f.** Average polymer length (including both linear and ring) at a large time as a function of κ. **g.** Average length of only linear chains at a large time as a function of κ. **h.** Average total number of monomers belonging to rings $M_{rings} = N_{rings} \times \langle l_{rings}(t \gg 1) \rangle$ at large simulation time. Note that some some simulations may not display any rings, in turn bringing the average M_{rings} below 1. MC = "Monte Carlo"; MD = "Molecular Dynamics".

employed in DNA looping [5, 33], our cyclisation parameter is more naturally interpreted as the number of rings formed for every two linear chains that are fused together. Intuitively, this number determines the final topological composition of the system. At $\kappa \gg 1$, we expect the final state of the system to be dominated by rings, while for $\kappa \ll 1$ to be dominated by linear chains. Importantly, since $k_0 \sim \langle l(t) \rangle^{-4\nu}$ the probability of ring formation decreases in time as the average length of the linear chains increases. Accordingly, and in spite of the fact that our system has a ring-only irreversible absorbing state, we conjecture that the strongly decreasing looping probability may effectively yield a very long time-transient in which the system is dominated by entangled linear chains with circular contaminants.

Since we expect the Smoluchovski equation to be valid only in the limit of low density where three-body interactions are negligible, the values of κ_0 and κ_1 should be independent on concentration only when c is small enough. By plotting $\kappa \equiv 2\kappa_0/(n_0\kappa_1)$ as a function of c/c^* (where c^* is computed at the beginning of the simulation or experiment) we show that κ scales as $n_0^{-1} \sim (c/c^*)^{-1}$ in both simulations and experiments until $c \simeq c^*$ where it starts to deviate (Fig. 2a); this confirms that the Smoluchovski approximation is valid in this range of concentrations. Importantly, in Fig. 2a we also identify the crossover value $\kappa = 1$ (at which the initial cyclisation rate is larger than the dimerisation rate) around $c/c^* \simeq 0.1 - 0.2$. We note that the agreement be-

tween simulations and experiments is excellent for small c/c^*. Quantitative analysis of gel electrophoresis images at larger c/c^* is challenging due to the poor separation of multimeric bands.

Runaway Transition – The results in Fig. 1 suggest that at large c/c^* the chains tend to grow longer, thus suppressing cyclisation; at the same time, the density of reactive ends and the speed of spatial exploration of the chains become smaller, thus suppressing dimerisation. Due to this kinetic competition, we ask whether the system can truly display a "runaway" phase, defined as a regime where at least one chain permanently escapes cyclisation and diverges in time. In Fig. 2b-c one can visually appreciate that at large reaction time, rings (blue) are abundant at low c/c^* while linear chains (grey) are more abundant at large c/c^*. Using a network representation (where monomer are converted into nodes and ligation events into edges) we also show that these systems display qualitative different network topologies (insets of Figs. 2b-c). At small c/c^* (large κ) the network of monomers is mostly disconnected; accordingly, even when the fraction of unreacted bonds goes to 0 at $t \to \infty$, the average length of the polymers does not diverge. On the contrary, at larger c/c^* we observe only few rings and some very large chains with very low cyclisation probability. A natural quantification is obtained by measuring the fraction of nodes in the giant connected component (GCC), i.e. the largest cluster of connected monomers corresponding to the longest chain in the system. At
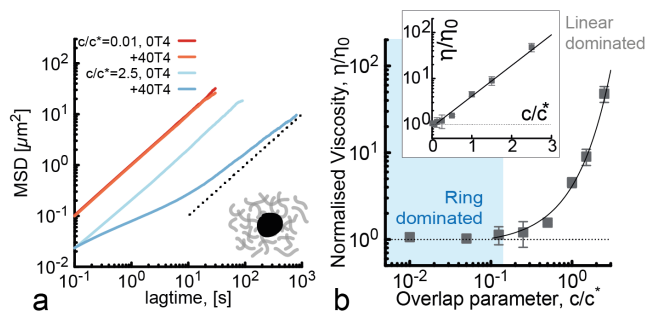
FIG. 3. **Rheological consequences of the runaway transition. a.** Mean squared displacements (MSDs) of 800 nm PVP-coated polystyrene beads diffusing in solutions of DNA. We compare the MSDs in solutions treated for 1 week either with 40U T4 ligase or buffer (control). **b.** Viscosity of the ligated solutions η, normalised by the viscosity of the control η_0. The inset shows the same plot in log-linear scale to highlight the exponential increase.

$\kappa = 1$ the GCC displays a change in scaling, growing as $GCC \sim \kappa^{-1} \sim c/c^*$ as $\kappa \to 0$ (Fig. 2e) suggesting that a change in behaviour takes place around $\kappa \simeq 1$.

Since MD simulations are computationally expensive, we employ Direct Simulation Monte Carlo (DSMC) [36–38] to solve the Smoluchowski equation and reach larger system sizes up to 10^5 chains (see SI). In Fig. 2f, we plot the number averaged chain length at an arbitrarily large time when the DSMC code has evolved the system as long as possible and has generated only a single linear chain accompanied by a number of rings. This figure suggests that the linear-dominated regime ($\kappa < 1$) displays an average polymer length at large reaction time that scales as $\langle l(t \gg 1) \rangle \sim \kappa^{-1} \sim c/c^*$. At the same time, the number average length of the *linear* population appears to reach a plateau that scales with the system size (Fig. 2g), indicating a runaway transition at $\kappa \lesssim 1$. Additionally the fraction of mass "lost" in forming rings decays as $f_{\mathrm{ring}} \sim \kappa$ and is thus negligible for small enough κ (Fig. 2h).

Although our simulations support the notion that a low value of κ will result in linear chains of increasing lengths and vanishing cyclisation rate, they are fundamentally limited to finite-size systems where the cyclisation rate of the largest chain never rigorously goes to 0. To firmly establish the existence of our runaway transition, in the SI we use an asymptotic theory to analytically demonstrate that the mass fraction of linear polymers goes to a finite limit at $t \to \infty$ in a thermodynamic system. We find that the key condition to ensure the runaway transition to exist is that the cyclisation rate $k_0 = \kappa_0 l^\mu$ decays strongly enough. More specifically, we require the exponent μ to be $\mu = -4\nu < -4\alpha/5$ or $\nu > \alpha/5$. This condition is always met in the Rouse unentangled ($\alpha = 1$) regime, and also in the entangled ($\alpha = 2$) regime, provided that the polymers are not fully collapsed ($\nu = 1/3$).

Dynamics – To test the consequences of the runaway transition on the dynamics, we perform microrheology experiments (see SI for details) where we track the dynamics of 800 nm PVP-coated polystyrene beads added

in a solution of DNA that has been treated with either 40U T4 ligase for a week (and thus to full extent of reaction) or with buffer for a week (control). At low concentrations, we observe that the mean squared displacement of the tracer particles $MSD(\tau) = \langle r(t + \tau) - r(t) \rangle$ is unaffected by the ligation of the DNA (Fig. 3a). On the contrary, for $c/c^* \geq 0.1$, we see that the MSDs of the tracers in the ligated systems are much slower and displays a stronger subdiffusive behaviour than the control (Fig. 3a). From the MSD, we extract the large-time diffusion coefficient D of the tracers and in turn the effective viscosity of the sample via the Stokes-Einstein equation [39]. The plot of the normalised viscosity (Fig. 3b) suggests that a dynamical transition takes place around $c/c^* = 0.1 - 0.2$ (or $\kappa \simeq 1 - 2$) which matches the structural runaway transition seen before (Fig. 3e-h).

After the transition, the viscosity increases exponentially with the concentration (see inset of Fig. 3b). This suggests a relaxation process dominated by end-retraction [35], possibly due to the threading of very long linear chains through small rings [13, 20, 40–42] or through pseudo-knotted parts of their own extremely long contour [43, 44]. We note that, especially at large c/c^*, the ligated solutions extremely elastic and the passive tracers do not display a freely diffusive behaviour even after a lag time of ten minutes. We thus argue that the reported η/η_0 may be lower bounds at large c/c^*, which would render the transition even more dramatic. All this implies that, intriguingly, near the transition $c/c^* \simeq 0.1$, systems prepared at similar concentrations may display extremely different rheology at large condensation times.

Conclusions – We have studied a system of chains undergoing irreversible condensation in competition with cyclisation. We have shown that the key adimensional parameter controlling growth kinetics is $\kappa = 2\kappa_0/(n_0\kappa_1)$; naturally interpreted as the number of rings formed for any one dimerisation. At large concentrations (or $\kappa < 1$) dimerisation is kinetically favoured and drives the growth of linear chains. While growth disfavours cyclisation, it also reduces the number of available reactive ends and the annealing rate of the chains (see Eq. (2)), disfavouring further growth. In spite of this, we discover that the net result of this kinetic competition is a runaway transition for $\kappa < 1$ if the cyclisation rate decays strongly enough with polymer length, i.e. with $\nu > \alpha/5$. In these conditions, the fraction of monomers transformed into rings is finite and small, thus leaving the rest of the monomers available to form a permanently growing linear chain. Finally, we discover that the runaway transition has deep consequences on the rheology, and triggers an exponential increase for $\kappa < 1$ (or $c/c^* > 0.1$).

Our results suggest that it may be possible to tune the final topological composition of ligated systems by judiciously choosing c/c^*. For instance, the most likely regime to form large rings and ring-linear blends [13, 41] is near the transition $c/c^* \simeq 0.1$. Mixing polymer families with different reactive ends further enhances the

designability as it introduces different c^* for each family. Interestingly, our results also suggest that Olympic gels [22, 45, 46] are unlikely to form during homopolymer condensation as they would require $c/c^* \gtrsim 1$ where loop formation is not favourable. Our results can also inform more efficient ways to perform genomic engineering, e.g., cloning of plasmids ought to be done at $c/c^* < 0.1$ whereas synthetic chromosome assembly at large c/c^*. Finally, it may be possible to couple dissipative DNA breakage reactions [47–49] with ATP-consuming ligation to create self-sustained and non-equilibrium solutions of topologically active polymers.

ACKNOWLEDGEMENTS

[1] M. Rubinstein and H. R. Colby, *Polymer Physics* (Oxford University Press, 2003).
[2] B. Alberts, A. Johnson, J. Lewis, D. Morgan, and M. Raff, *Molecular Biology of the Cell* (Taylor & Francis, 2014) p. 1464.
[3] P. J. Flory, Journal of the American Chemical Society **58**, 1877 (1936).
[4] M. E. Cates and S. J. Candau, EPL **55**, 887 (2001).
[5] T. Vafabakhsh Reza, Ha, Science **337**, 1097 (2012).
[6] H. Zhou, J. Woo, A. M. Cok, M. Wang, B. D. Olsen, and J. A. Johnson, Proc. Natl. Acad. Sci USA **109**, 19119 (2012).
[7] M. Lang and K. S. Kumar, Macromolecules **54**, 7021 (2021).
[8] S. Di Stefano and L. Mandolini, Physical Chemistry Chemical Physics **21**, 955 (2019).
[9] P. J. Flory and J. A. Semlyen, Journal of the American Chemical Society **88**, 3209 (1966).
[10] C. Madeleine-Perdrillat, F. Delor-Jestin, and P. De Sainte Claire, Journal of Physical Chemistry B **118**, 330 (2014).
[11] H. R. Kricheldorf, S. M. Weidner, and F. Scheliga, Polymer Chemistry **11**, 2595 (2020).
[12] H. Jacobson and W. H. Stockmayer, The Journal of Chemical Physics **18**, 1600 (1950).
[13] M. Kapnistos, M. Lang, D. Vlassopoulos, W. Pyckhout-Hintzen, D. Richter, D. Cho, T. Chang, and M. Rubinstein, Nature materials **7**, 997 (2008).
[14] A. Rosa and R. Everaers, Phys. Rev. Lett. **112**, 118302 (2014).
[15] J. D. Halverson, W. B. Lee, G. S. Grest, A. Y. Grosberg, and K. Kremer, The Journal of chemical physics **134** (2011).
[16] D. Tsalikis and V. Mavrantzas, ACS Macro Lett. **3**, 763 (2014).
[17] E. Lee, S. Kim, and Y. Jung, Macromol. Rapid Commun. **36**, 1115 (2015).
[18] D. Michieletto and M. S. Turner, Proc. Natl. Acad. Sci. USA **113**, 5195 (2016).
[19] T. C. O'Connor, T. Ge, M. Rubinstein, and G. S. Grest, Physical Review Letters **124**, 1 (2020).
[20] D. Parisi, J. Ahn, T. Chang, D. Vlassopoulos, and M. Rubinstein, Macromolecules **53**, 1685 (2020).
[21] E. Uehara and T. Deguchi, Journal of Chemical Physics **145** (2016).
[22] J. Fischer, M. Lang, and J. U. Sommer, Journal of Chemical Physics **143** (2015).
[23] A. Rosa, J. Smrek, M. S. Turner, and D. Michieletto, ACS Macro Letters **9**, 743 (2020).
[24] Y. Zhou, K. W. Hsiao, K. E. Regan, D. Kong, G. B. McKenna, R. M. Robertson-Anderson, and C. M. Schroeder, Nature Communications **10**, 1 (2019).
[25] J. Smrek, I. Chubak, C. N. Likos, and K. Kremer, Nature Communications **11**, 1 (2020).
[26] J. Smrek, J. Garamella, R. Robertson-Anderson, and D. Michieletto, Science Advances **7**, 1 (2021).
[27] K. R. Peddireddy, D. Michieletto, G. Aguirre, J. Garamella, P. Khanal, and R. M. Robertson-Anderson, ACS Macro Letters **10**, 1540 (2021).
[28] R. M. Ziff, Journal of Statistical Physics **23**, 241 (1980).
[29] K. Kremer and G. S. Grest, The Journal of Chemical Physics **92**, 5057 (1990).
[30] A. Bates and A. Maxwell, *DNA topology* (Oxford University Press, 2005).
[31] P. G. De Gennes, The Journal of Chemical Physics **76**, 3322 (1982).
[32] P. G. De Gennes, The Journal of Chemical Physics **76**, 3316 (1982).
[33] J. Shimada and H. Yamakawa, Macromolecules **17**, 689 (1984).
[34] A. Rosa, N. B. Becker, and R. Everaers, Biophys. J. **98**, 2410 (2010).
[35] M. Doi and S. Edwards, *The theory of polymer dynamics* (Oxford University Press, 1988).
[36] A. L. Garcia, C. Van Den Broeck, M. Aertsens, and R. Serneels, Physica A **143**, 535 (1987).
[37] K. Liffman, J. Comput. Phys. **100**, 116 (1992).
[38] F. E. Kruis, A. Maisels, and H. Fissan, AIChE J. **46**, 1735 (2000).
[39] J.-P. Hansen and I. R. McDonald, *Theory of simple liquids: with applications to soft matter* (Academic press, 2013).
[40] J. Roovers, Macromolecules **21**, 1517 (1988).
[41] J. D. Halverson, G. S. Grest, A. Y. Grosberg, and K. Kremer, Phys. Rev. Lett. **108**, 038301 (2012).
[42] Y. Zhou, C. D. Young, M. Lee, S. Banik, D. Kong, G. B. McKenna, R. M. Robertson-Anderson, C. E. Sing, and

C. M. Schroeder, Journal of Rheology **65**, 729 (2021).

[43] D. Michieletto, D. Marenduzzo, E. Orlandini, G. P. Alexander, and M. S. Turner, Soft Matter **10**, 5936 (2014).

[44] B. W. Soh, A. R. Klotz, R. M. Robertson-Anderson, and P. S. Doyle, Physical Review Letters **123**, 1 (2019).

[45] Y. Diao, K. Hinson, R. Kaplan, M. Vazquez, and J. Arsuaga, J. Math. Biol. **64**, 1087 (2012).

[46] D. Michieletto, D. Marenduzzo, and E. Orlandini, Phys. Biol. **12**, 036001 (2015).

[47] D. Michieletto, P. Neill, S. Weir, D. Evans, N. Crist, V. A. Martinez, and R. M. Robertson-Anderson, Nature Communications **13** (2022), 10.1038/s41467-022-31828-w.

[48] E. Del Grosso, E. Franco, L. J. Prins, and F. Ricci, Nature Chemistry **14**, 600 (2022).

[49] L. Heinen and A. Walther, Science Advances **5**, 32 (2019).

Runaway Transition in Irreversible Polymer Condensation with Cyclisation: Supplementary Information

Maria Panoukidou,[1, *] Simon Weir,[1, *] Valerio Sorichetti,[2] Yair
Gutierrez Fosado,[1] Martin Lenz,[2, 3] and Davide Michieletto[1, 4, †]

[1]*School of Physics and Astronomy, University of Edinburgh,*
Peter Guthrie Tait Road, Edinburgh, EH9 3FD, UK
[2]*Laboratoire de Physique Théorique et Modèles Statistiques (LPTMS),*
CNRS, Université Paris-Saclay, F-91405 Orsay, France
[3]*PMMH, CNRS, ESPCI Paris, PSL University, Sorbonne Université, Université de Paris, F-75005, Paris, France*
[4]*MRC Human Genetics Unit, Institute of Genetics and Cancer,*
University of Edinburgh, Edinburgh EH4 2XU, UK

METHODS

Molecular Dynamics Simulations

Force-Field and equilibration process

We model a 6,500 bp-long linear DNA molecule as a bead-spring polymer made of $l_0 = 174$ beads. The total number of polymer chains is $N_m = 200$. The polymers are modelled *via* the Kremer-Grest model [1]. Each bead has a diameter $\sigma = 13$ nm (or ~ 38 bp), modelled as a truncated and shifted Lennard-Jones potential (WCA)

$$U_{\text{LJ}}(r) = 4\epsilon \left[(\sigma/r)^{12} - (\sigma/r)^6 + 1/4\right], \tag{1}$$

for $r < r_c = 2^{1/6}\sigma$ and 0 otherwise. Here r represents the distance between beads and $\epsilon = 1.0$ parametrises the strength of the potential. The radius of the bead, σ, defines the length units in our system. Consecutive beads are connected through a permanent Finite Extensible Non-linear Elastic (FENE) bond

$$U_{\text{FENE}}(r) = -0.5KR_0^2 \log\left[1 - (r/R_0)^2\right] \tag{2}$$

with $K = 30\epsilon/\sigma^2$ and $R_0 = 1.5\sigma$. The bending stiffness of the polymer is controlled by a Kratky–Porod interaction

$$U_b(r) = \frac{k_B T l_p}{\sigma}(1 - \cos\theta), \tag{3}$$

which regulates the angle (θ) defined by the two tangent vectors connecting three consecutive beads along the polymer. Here, $l_p = 4\sigma = 150$ bp is the persistence length of DNA. The solvent is simulated implicitly using a Langevin thermostat, so that the time evolution of our system is governed by the stochastic partial differential equations

$$m\ddot{\boldsymbol{r}} = -\xi\dot{\boldsymbol{r}} - \boldsymbol{\nabla}U + \sqrt{2k_B T\xi}\boldsymbol{\eta} \tag{4}$$

---

* joint first author
† corresponding author, davide.michieletto@ed.ac.uk

where $\boldsymbol{r}$ is the position of a particle, ξ its friction, m its mass, U the sum of the interaction potentials discussed above and $\boldsymbol{\eta}$ white noise with unit variance. The diffusion timescale is $\tau_B = \xi\sigma_b^2/k_B T$. The integration of the Langevin equation is done with a velocity-Verlet algorithm, using a time step $\Delta t = 0.012\tau_B$ in LAMMPS [2].

Various monomer densities were considered, ranging from $10^{-2}c^*$ to $1c^*$, where $c^* = 0.012\sigma^{-3}$ is the monomer concentration at which the polymers start to overlap. The overlap concentration c^* was measured by computing the radius of gyration R_g of the polymers in equilibrium at very large dilution ($c^* = l_0/(4/3\pi R_g^3)$). All the systems were equilibrated for a sufficient amount of time to ensure that the polymer chains have moved at least a distance equal to R_g.

Topology reconstruction

After the equilibration step, 40 replicas of production runs were started for each monomer number density considered. The ligation is performed stochastically, and is attempted every 100 time steps between two polymer end beads that are closer than $R_c = 2^{1/6}\sigma$ using the `fix bond/create` LAMMPS command. The probability of successful ligation (i.e., bond formation) is set to $f = 0.1$. Once ligated, the bond formed between the polymers is irreversible and cannot be broken, therefore accounting for the formation of a covalent bond between the DNA fragments. During the ligation process snapshots of the system are taken every 10^6 time steps on both the 3D coordinates of the beads and the bond list at those time steps. From the bond list we can, later on, reconstruct the topology of the individual polymers, i.e. if fused with others to form linear chains or if circularised.

Once the production runs finished, the trajectories were analysed and the topology was reconstructed using our python code (https://git.ecdf.ed.ac.uk/taplab/dna-ligation.git). We will refer to this code from now on as TR code. The code takes as input the instantaneous trajectory and bond list from LAMMPS and checks for newly formed linear and ring chains. The output of the python code is a file containing the number and length of linear chains that have formed in a

given simulation time step. Similar files are produced for the ring chains. These files are then used to calculate the average length and the number of linear/ring chains figures.

The starting point of the topology reconstruction algorithm is an array $\mathbf{b}$ of size $N_b \times 2$; each row $b_i = (id_1, id_2)$ represents the IDs of atoms that are bonded within the system:

$$\mathbf{b} = \begin{bmatrix} id_1 & id_2 \\ id_3 & id_4 \\ \vdots & \vdots \\ id_{N_{n-1}} & id_{N_n} \end{bmatrix},$$

Since not all particles are linked together, some do not appear in the array $\mathbf{b}$. In order to avoid operations with large sparse arrays, the matrix $\mathbf{b}$ is mapped to $\tilde{\mathbf{b}}$ that contains only indexes from 1 to the maximum number of atoms connected $M : \mathbf{b} \to \tilde{\mathbf{b}}$.

The next step of the TR algorithm is to create a connectivity matrix $\mathbf{C}$ based on the list $\tilde{\mathbf{b}}$. Each row of $\mathbf{C}$ represents an atom index and consists of three components $\mathbf{C}(id_i, :) = (id_{i-1}, id_{i+1}, flag)$. Since in our case a particle can be linked with two more particles the first two components of each row id_{i-1}, id_{i+1} represent the connections of particle id_i (note that id_{i-1} and $id + i + 1$ are not necessarily consecutive in 1D but can be any other particle bonded to particle i). The third component, $flag$, takes only the values $0, 1$ and accounts for the particles id_i that already belong to a polymer chain. The flag column of $\mathbf{C}$ is initialised to zeros. During the reading process of the connectivity matrix the algorithm switches the flags to 1 of the particles that are already considered to belong in a chain. Rings are extracted in the same manner and a ring is found if the current atom index is the same as the starting atom index. This reading process outputs N_c arrays which have different lengths and each of them contains the particle (mapped) ids that are connected in a polymer chain. The final step of the TR algorithm is to map the atom indexed back to the original ones: $M^{-1} : \tilde{\mathbf{b}} \to \mathbf{b}$. This algorithm is very generic and can be applied also in cases where the atoms are not initially in polymers as in our case, but rather individual atoms that can connect with each other during the simulation.

Experiments

We consider a 6500 bp-long plasmid (referred to as 1288 here) which is converted into linear form by using a restriction enzyme (XhoI). This linearisation step is checked on a gel electrophoresis. The equilibrium radius of gyration of this linear DNA molecule is about $R_g \simeq l_p\sqrt{L/3l_p} \simeq 0.2$ μm (in agreement with diffusion data from Ref. [3]). This yields an overlap concentration $c^* = 3M/(4N_A\pi R_g^3) \simeq 0.2$ mg/ml where

$N_A = 6.023\,10^{23}$ 1/mol is the Avogadro number and $M = L \times 650$ g/mol is the molecular weight of the plasmid. For the low DNA concentration experiments we set ourselves at $0.01c^*$, i.e. $c = 2$ μg/ml. To perform ligation we use T4 ligase (NEB, M0202L, 1U corresponds to 0.5 ng or 0.00735 pmoles of protein according to Ref. [4]), and work at 1x T4 ligase reaction buffer concentration, which contains 1 mM ATP.

To classify the topology of the DNA under ligation, we perform time-resolved gel electrophoresis. We prepare a master solution of DNA at desired concentration, 1x ligase buffer and 2 U/μl T4 ligase. Aliquots are taken at different elapsed times, the T4 ligase is heat-inactivated at 65° for 15 minutes. Aliquots are treated with Nb.BbvCI Nickase (NEB, R0631L) to relax the supercoiled population. A subaliquot is created and treated with exonuclease (PlasdmiSafe, Lucigen) to remove the linear population. The resulting aliquots are run on a gel: we load 20ng of DNA from each aliquot onto a 1% agarose gel prepared using 1x TAE buffer. A standard λDNA - HindIII digest (NEB,N3012S) marker is also loaded. The gel is run at ~ 2.5V/cm for 5 hours and post-stained with Sybr-Gold (ThermoFisher) for 30 minutes. A Syngene G-box and Genesys software is used to image the gels.

The combination of nickase (relaxing the DNA supercoiling) and exonuclease (fully digesting linear DNA molecules) allowed the topology of the DNA in each band to be unambiguously identified. Further, the λDNA - HindIII digest marker confirmed the bands were of the correct size for monomer and dimer lengths. To extract the relative amount of molecules in each lane we compute, using ImageJ, the intensity of each lane and account for the fact that the band with dimers has chains that are twice as long. We then normalise against the sum of the three bands to obtain the relative fraction of chains in each population.

The dynamics of the systems are measured using microrheology. Solutions are made by mixing 8 μl of 1288 linearised plasmid at different concentrations to a final concentration in the range 2ng/μl-500ng/μl with 1 μl of 40 U/ul T4 ligase and 1 μl of T4 ligase reaction buffer. Control solutions are prepared at the same time and in the same manner substituting additional TE for the T4 ligase. The samples are kept at room temperature on a roller for several days. The samples are then spiked with $a = 800$ nm PVP-coated polystyrene beads, pipetted and sealed onto a slide and imaged using an inverted microscope. We take a 30-minute movie and we analyse the movies using a particle tracking algorithm (trackpy [5]) and extract the trajectories and mean squared displacements(MSD) of the tracers $\langle \Delta r^2(t) \rangle = \langle [\boldsymbol{r}(t + \tau) - \boldsymbol{r}(t)]^2 \rangle$. Diffusion coefficients are extracted by fitting to the MSD's via MSD$= 2Dt$. The viscosity is obtained using the Stokes-Einstein relation [6], $\eta = k_B T/(3\pi Da)$.

GENERIC CONSIDERATIONS ON THE PROPOSED SMOLUCHOWSKI EQUATION

In this section we explain in detail how we solve the modified Smoluchowski equation reported in the main text. The linear polymers undergo irreversible ligation with rate $k_1(i,j)$ (i,j=lengths of the filaments reacting) and cyclisation with rate $k_0(l)$. The concentrations of filaments of length l at time t, $\rho(l,t)$, and of rings, $\rho_r(l,t)$, are thus governed by the following equations:

$$\dot{\rho}(l,t) = \frac{1}{2} \sum_{ij;i+j=l} k_1(i,j)\rho(i,t)\rho(j,t)+$$

$$- \rho(l,t) \sum_{i=1}^{\infty} k_1(l,i)\rho(i,t) - k_0(l)\rho(l,t) \quad (5)$$

$$\dot{\rho}_r(l,t) = k_0(l)\rho(l,t) . \quad (6)$$

Once a chain undergoes cyclisation, it cannot react anymore and thus is removed from the ensemble of linear chains and transferred to the ensemble of rings. The dynamics is also constrained by the requirement that no monomers are created or destroyed and the total mass is conserved:

$$\sum_{l=1}^{\infty} l[\rho(l,t) + \rho_r(l,t)] = N/V = n \quad \forall t \quad (7)$$

where N is the total number of monomers and V is the system's volume. Assuming that the reaction takes place on a time scale larger than the Rouse relaxation time, the length-dependence of the annealing rate is [7]

$$k_1(i,j) = \kappa_1(D_i + D_j)(R_i + R_j) \quad (8)$$

$$= \kappa_1 \left(l_i^{-\alpha} + l_j^{-\alpha} \right) \left(l_i^{\nu} + l_j^{\nu} \right) , \quad (9)$$

where κ_1 is a constant coefficient and $l_i = il_0$ is the length of a polymer with degree of polymerisation i, with l_0 the monomer size. The cyclisation rate is taken to be $k_0(l) = \kappa_0 l^{\mu}$, where $\mu = -4\nu$. Note that we take $\mu = -4\nu$ instead of the Shimada-Yamakawa exponent $\mu = -3\nu$ because we are dealing with a non-equilibrium, subdiffusive search process (see below). As we describe in detail later (see "Looping probability and the exponent μ" section), both theory and simulations suggest that the *irreversible* looping probability scales with the length of the chain as $l^{-4\nu}$ and not as $l^{-3\nu}$.

Time scaling of the mean length - concentrated regime

We can solve the Smoluchovski equation in the concentrated limit, where we expect the ring formation to be negligible. We can thus use a mean-field expression for the mean length l and estimate (at scaling level) the rate as

$$k \sim DR \sim l^{\nu-\alpha} . \quad (10)$$

The timescale of chain growth is related to this rate and, in a mean-field picture, we can write $d\rho(t)/dt = -k\rho(t)^2$ or

$$k \sim \frac{1}{\rho(t)t} \quad (11)$$

according to dimensionality arguments. In these equations, $\rho(t)$ is the number density of chains with mean length l. This also means that

$$t \sim \frac{1}{\rho(t)k} \sim \frac{l^{-\nu+\alpha}}{\rho(t)} . \quad (12)$$

We now point out that the average number of fragments is related to the average length of the fragments as $\rho(t) = l_0\rho(0)/l$. This is because mass is conserved so $\rho(0)l_0 = \sum_i \rho_i(t)(il_0)$, or in mean field, $\rho(0)l_0 = \rho l$ at any time. Hence we find

$$t \sim \frac{1}{\rho(t)k} \sim \frac{l^{-\nu+\alpha}}{\rho(t)} \sim \frac{l^{-\nu+\alpha+1}}{\rho(0)l_0} \sim l^{1+\alpha-\nu} . \quad (13)$$

To find how the mean length grows in time we can just invert this equation to find

$$l(t) \sim t^{1/(1+\alpha-\nu)} \sim t^{1/(1-\lambda)} \equiv t^{\gamma} , \quad (14)$$

with $\lambda = \nu - \alpha$. Notice that $\alpha = 1$ for Rouse dynamics and $\alpha = 2$ for reptation. Recall that here we are considering the diffusion in 3D of the chain, not its curvilinear diffusion, hence why $\alpha = 2$ for reptating chains. At the same time, we consider $\nu = 1/2$ for ideal chains and $\nu = 3/5$ for self-avoiding chains. For instance, by plugging in these numbers we obtain $l \sim t^{\gamma}$ with $\gamma \simeq 0.66 - 0.7$ for Rouse (so above overlap but not entangled) and $\gamma \simeq 0.4$ for reptation (so above overlap and entangled).

Time-dependence of the mean length - dilute regime

In the very dilute regime, we can assume that rings and short n-mers should be more favourable. We thus now solve the Smoluchovski equation analytically assuming that only monomers, dimers and monomer rings are present. Let us assume that the concentration of rings, monomers and dimers is denoted by n_r, n_1 and n_2, respectively. The dynamical system that describes the evolution of those populations is the following:

$$\frac{dn_r(t)}{dt} = k_0(1)n_1(t) \quad (15)$$

$$\frac{dn_1(t)}{dt} = -k_1(1,1)n_1^2(t) - k_0(1)n_1(t) \quad (16)$$

$$\frac{dn_2(t)}{dt} = \frac{1}{2}k_1(1,1)n_1^2(t) \quad (17)$$

We solve Eq. (16) neglecting the second term as $n_1^2 \ll 1$ in the infinite dilution limit:

$$n_1(t) = n_1(0)e^{-k_0(1)t} \quad (18)$$

The concentration of monomer rings is thus

$$\frac{dn_r(t)}{dt} = k_0 n_1(0) e^{-k_0(1)t} \qquad (19)$$

which yields

$$n_r(t) = n_1(0)(1 - e^{-k_0(l)t}). \qquad (20)$$

Substituting in Eq. (17), we get

$$\frac{dn_2(t)}{dt} = \frac{1}{2}k_{11}n_1^2(t) = \frac{1}{2}k_{11}\left(n_1(0)e^{-k_0(1)t}\right)^2 \qquad (21)$$

which yields

$$n_2(t) = \frac{1}{4k_0}k_{12}n_1^2(0)\left(1 - e^{-2k_0(1)t}\right). \qquad (22)$$

Assuming these three are the only contributions to the system, then the mean length is given by the following relation

$$\langle l(t) \rangle = \frac{l_0 n_1(t) + l_0 n_o(t) + 2l_0 n_2(t)}{n_1(t) + n_o(t) + n_2(t)} =$$
$$= l_0 \frac{n_1(t) + n_o(t) + 2n_2(t)}{n_1(t) + n_o(t) + n_2(t)}. \qquad (23)$$

In denser solutions, where the population is more polydisperse, the Smoluchowski equation cannot be solved analytically and we refer to the previous section for a scaling prediction and in the section "Looping probability and the exponent μ" for a perturbative approach in the limit of small cyclisation. In the next section we explain the numerical method that we implement to solve it.

Time-dependence of the mean length - concentrated regime

To numerically solve the Smoluchowski equation Eq. (6) we wrote a code in MATLAB using the explicit Euler scheme. The numerical evaluation of Eq. (6) is then iterated to find the best free parameters κ_0 and κ_1 that fit the MD or experimental mean length versus time data. We recall the expression of the ligation rate: $k_1(i,j) = \kappa_1[(il_0)^\nu + (jl_0)^\nu][(il_0)^{-\alpha} + (jl_0)^{-\alpha}]$ and of the cyclisation rate $k_0(l) = \kappa_0 l^\mu$. The fit is done using the nonlinear least squares MATLAB embedded function (i.e. lsqcurvefit). The rate of ring formation κ_0 and the rate of linear chains formation κ_1 are extracted from this fit by considering four independent sets of 10 independent simulations replicas so that we obtain an error on the fits.

Solving the Smoluchowski equation to fit the data from MD simulations consists of two main parts:

1. We create an objective function for the lsqcurvefit (called Obj_smoluchowski) that takes as input the array of initial coefficient guess $K_0 = (\kappa_1, \kappa_0)$ and the time data array *xdata*. It returns the average length as a function of time, array *ydata*. In the objective function:

(a) An array $\mathbf{L} = \mathbf{n} \cdot N_0$ is initialised where $n = \{1, 2, \ldots, N_m = 200\}$ and $N_0 = 174$. This represents the set of lengths that can be found in the system (recall that we initialise our MD simulations with 200 chains of 174 beads each). Also, the arrays with the number density of linear and ring chains are initialised as follows, $\mathbf{n_{l_0}} = (N_m/vol, 0, \ldots, 0)_{1 \times N_m}$ and $\mathbf{n_{r_0}} = (0, \ldots, 0)_{1 \times N_m}$ since initially all the molecules are linear chains.

(b) *for* $t = \{1$ to simulation final step time$\}$ do *call* $(\mathbf{n_{L_{new}}}, \mathbf{n_{R_{new}}}) = exEuler\_smoluchowski(\mathbf{n_L}, \mathbf{n_R}, K)$ function (see point 2 below)

(c) update arrays $\mathbf{n_L} = \mathbf{n_{L_{new}}}$ and $\mathbf{n_R} = \mathbf{n_{R_{new}}}$. Calculate the total average length $\mathbf{l_{total}}$ as

$$\mathbf{l_{total}(t)} = \frac{\mathbf{n_{L_{new}}} \cdot \mathbf{L} + \mathbf{n_{R_{new}}} \cdot \mathbf{L}}{\sum_i^{N_m} n_{L_{new}}^i + \sum_i^{N_m} n_{R_{new}}^i}$$

(d) *exit for loop* and parse $\mathbf{l_{total}(t)}$ to *ydata*

2. The exEuler_smoluchowski function takes as input the initial number densities of linear and ring chains and the reaction rates $\mathbf{n_L}, \mathbf{n_R}, K$. Based on the given rates K, it outputs final number density arrays $\mathbf{n_{L_{new}}}, \mathbf{n_{R_{new}}}$, after the reactions have taken place. When this function is called, the number density of linear and ring chains of each population are updated according to Eq. (6). The monomer, dimer, and so on populations are increased according to the first two terms of Eq. (6) while the number of them that is converted into rings is subtracted by the $\mathbf{n_{L_{new}}}$ and added to the $\mathbf{n_{R_{new}}}$ array.

In the first two terms of Eq. (6) the rate $k_1(i,j)$ is not a scalar quantity by rather a matrix that follows the relation Eq. (9). The extracted coefficient against which the fitting is optimised is the scalar κ_1. Similarly, for the sink term of Eq. (6), the equation $k_0(l) = \kappa_0 l^{-4\nu}$ is used and the fitting coefficient exported is the scalar κ_0.

The coefficients $K = (\kappa_1, \kappa_0)$ are updated iteratively by the lsqcurvefit algorithm to best fit the data. Once the optimum values are obtained the algorithm terminates.

Looping probability and the exponent μ

In equilibrium the looping probability of a chain of length L is given by the Shimada-Yamakawa formula [8, 9]. For $L \gg l_p$ (with l_p the persistence length) the looping probability decays as $P(L) \sim L^\mu$ with $\mu = -3\nu$. This looping probability also holds for an irreversible, non-equilibrium scenario if the process is reaction-limited. This is because the chain ends would have the time to explore many conformations and to diffuse the whole
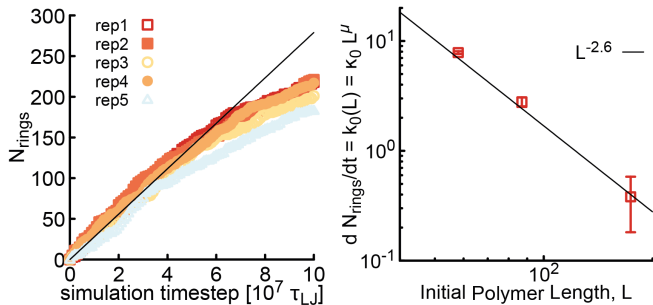
FIG. 1. Computing the rate of loop formation as a function of polymer length. (Left) N_{rings} as a function of time for a system with $N_0 = 400$ chains with $M = 87$ monomers each. The black line represents the average of the numerical derivatives of the curves in the limit $t \to 0$. (Right) Numerical derivative dN_{rings}/dt showing a power law decay as a function of initial polymer length. The exponent of the power law is found to be -2.6, close to the values -4ν which matches our calculation assuming the irreversible loop formation to be a diffusion-limited and sub-diffusive search process (see text).

volume of the chain, $V \sim L^{3\nu}$, before reacting (as it would happen in equilibrium). In a diffusion-limited, irreversible ligation process, one should instead compute the time it takes for an end to diffuse over a certain length distance ξ. The dynamics of the end is described by the Rouse model [10], so that $\xi = b(D_1 t/b^2)^{1/4}$, where b is the size of a monomer and D_1 its free diffusion coefficient. Then, setting $\xi = R$ (the size of the chain) one obtains $(R/b)^4 = (D_1 t/b^2)$, which implies $k_0 \sim t^{-1} \sim R^{-4} \sim L^{-4\nu}$. So considering $\mu = -4\nu$ effectively takes into account the fact that the chain ends are performing a sub-diffusive search process within the polymer coil, as expected for Rouse dynamics.

We have used MD simulations to check the dependence on the polymer length of our loop formation. To do this we ran short dilute simulations and starting from polymers with different lengths, monitored the number of rings N_{rings} over time and then taken the derivative dN_{rings}/dt in the limit $t \to 0$. As shown in Fig. 1, the rate of ring formation $dN_{\text{rings}}/dt = k_0(L) = \kappa_0 L^\mu$ follows a power law which we can fit with an exponent that is close to $\mu = -4\nu$, with $\nu = 0.588$ the exponent expected for self-avoiding chains. In light of this evidence, we decided to use $\mu = -4\nu$ in the main paper.

CALCULATION OF MASS CONVERTED INTO RINGS AT INFINITE TIME

To estimate the amount of mass that is converted into rings at long times, we do a perturbative calculation valid in the limit of small κ. We start from the continuum

Smoluchovski equation:

$$\frac{d\rho(l,t)}{dt} = \frac{1}{2}\int_0^l K(i,l-i)\rho(i,t)\rho(l-i,t)di +$$
$$- \int_0^\infty K(i,l)\rho(l,t)\rho(i,t)di - \frac{1}{2}\kappa l^\mu \rho(l,t), \qquad (24)$$

where we define $K \equiv k_1/\kappa_1$ and recall that $\kappa \equiv 2\kappa_0/(n_0\kappa_1)$ which is thus a scaling function such that $K(ai,al) \sim a^\lambda k_1(i,l)$ where $\lambda = \nu - \alpha$ [11].

We now treat κ_0 perturbatively, starting with $\kappa_0 = 0$. In this case, there is no mass lost into rings and we can thus write a conservation law

$$\int_0^\infty l\rho(l,t)dl = 1 \quad \forall t. \qquad (25)$$

Even for κ non zero, we assume the loss of mass to cyclisation remains finite and of order κ. We will check the self-consistency of this assumption below. Using the mass conservation and Eq. (24) we can write the following scaling relations: $l^2\rho = 1$, $\rho t^{-1} = l^{1+\lambda}\rho^2$. We therefore obtain:

$$l \sim t^{1/(1-\lambda)}. \qquad (26)$$

which is the same as Eq. (14). Note that we must have $\lambda < 1$ for the average length of polymers to increase over time. We can also write the density distribution as

$$\rho \sim t^{-2/(1-\lambda)} \qquad (27)$$

which in the limit of long times or large lengths may be written as

$$\rho(l,t) \sim t^{-2/(1-\lambda)}\mathcal{G}\left(\frac{l}{t^{1/(1-\lambda)}}\right) \qquad (28)$$

where $\mathcal{G}$ is a scaling function that only depends on the ratio $l/t^{1/(1-\lambda)}$.

We now introduce the ring length distribution $\rho_r(l,t)$ and its evolution equation as

$$\frac{d\rho_r(l,t)}{dt} = 2\kappa_0 l^\mu \rho(l,t). \qquad (29)$$

Since at time $t = 0$ there are no rings, we can then write

$$\rho_r(l,t \to \infty) = 2\kappa_0 l^\mu \int_0^\infty \rho(l,t)dt. \qquad (30)$$

We can plug in the result we obtained for the distribution of length of linear chains Eq. (28) to yield

$$\rho_r(l,t \to \infty) = 2\kappa_0 l^\mu \int_0^\infty t^{-2/(1-\lambda)}\mathcal{G}\left(\frac{l}{t^{1/(1-\lambda)}}\right)dt$$
$$= 2\kappa_0 l^\mu(1-\lambda)l^{-(1+\lambda)}\int_0^\infty x^{-\lambda}\mathcal{G}(x)dx \qquad (31)$$

where we defined $x = l/t^{1/(1-\lambda)}$. Thus, the number density of polymers that are converted into rings over infinite time is

$$\rho_r^\infty(l) = 2\kappa_0(1-\lambda)l^{\mu-1-\lambda}\int_0^\infty x^\lambda \mathcal{G}(x)dx. \quad (32)$$

Since $\lambda < 1$ and assuming the $\mathcal{G}(x) = \mathcal{O}(1)$ when $x \to 0$, the integral converges in 0. For convergence of this integral at ∞ we also require that the scaling function decays faster than $x^{\lambda-1}$.

Assuming this functional form for the distribution of ring lengths at infinite time, we now compute the total average mass transformed into rings at infinite time as

$$M_{\text{rings}}^\infty = \int_1^\infty l\rho_r^\infty(l,t)dl$$
$$= 2\kappa_0(1-\lambda)\int_0^\infty x^{-\lambda}\mathcal{G}(x)dx\int_1^\infty l^{\mu-\lambda}dl. \quad (33)$$

The convergence of this integral requires that $\lambda - \mu > 1$ and in this case we get

$$M_{\text{rings}}^\infty = 2\kappa_0\frac{1-\lambda}{\lambda-\mu-1}\int_0^\infty x^{-\lambda}\mathcal{G}(x)dx. \quad (34)$$

From this equation we see that the fraction of mass in rings at infinite time $M_{\text{rings}}^\infty/M_0$ converges to a finite value proportional to κ_0 (and hence < 1 at small κ_0).

With this calculation we have thus shown that at small enough but non-zero κ_0, the fraction of mass turning into rings is finite if $\lambda - \mu = \nu - \alpha + 4\nu > 1$ or $\nu > \alpha/5$ which is valid for any type of polymer in the non-entangled ($\alpha = 1$) regime, and for ideal and self-avoiding polymers in the entangled regime ($\alpha = 2$). This implies that in these regimes we expect the cyclisation probability to decay fast enough and cannot prevent the runaway of the $M_0 - M_{\text{rings}}^\infty$ mass into linear chains that keep growing in time.

Consistently with this, in both MD and MC simulations we never observe the formation of rings larger than 10 initial monomers.

DESCRIPTION OF THE DSMC ALGORITHM

The modified Smoluchowski equation proposed here (6) can only be solved analytically for certain forms of the ligation rate $k_1(i,j)$ and of the cyclisation rate $k_0(l)$. Moreover, the computational cost of directly solving the system of ordinary differential equations as described in Sec. increases steeply with the system size. Thus, in order to find solutions to the Smoluchowski equation for larger system sizes, we employ here Direct Simulation Monte Carlo (DSMC) [12–14]. DSMC is a powerful stochastic method to solve differential equations such as Eq. (6), and which samples the correct ligation kinetics in the limit of large system sizes. The starting point for the Monte Carlo algorithm is an array $\mathbf{m}$ of length N, each element i of which contains a number m_i which represents the mass/length of the chains i:

$$\mathbf{m} = (m_1, m_2, \ldots, m_N).$$

A value of 0 corresponds to absence of a certain chain. Moreover, to satisfy mass conservation we ensure that $\sum_{i=1}^N m_i = N$ (total number of monomers) is true for any time during the simulation. We will also consider an analogous array of length N denoted $\mathbf{r}$ (initially empty), where we save the masses of the rings.

For an initially monodisperse condition, we set $\mathbf{m}_0 = (1, 1, \ldots, 1)$. After the array $\mathbf{m}$ is initialized, we run the DSMC simulation, which consists in repeating a large number of times a Monte Carlo step (described below). The execution is terminated when the the system has reached a state in which there is a single linear chain and a number of non-reactive rings.

Description of the Monte Carlo step

In this paragraph, we will describe the single Monte Carlo (MC) step, which is repeated a large number of times during the numerical resolution of Eq. (6) performed using the DSMC algorithm. With reference to Eq. (6), we define $n_f \equiv V\sum_{i=1}^\infty n_i$ (total number of chains). Before the start of the simulation, we give an estimate of the maximum annealing rate $k_{\max}$ and of the maximum cyclisation rate $k_0^{\max}$. The exactness of the algorithm does not depend on this initial choice, however, choosing values that are too far from the actual maximum rates can lead to a reduced efficiency [12].

During every MC step, we either attempt to perform an ligation reaction (with probability p) or a cyclisation one (with probability $1 - p$). The value of p is calculated initially and then updated during the course of the simulation in such a way that the average number densities $n(l)$ satisfy (6). At the beginning of each MC step, p is evaluated as

$$p^{-1} = 1 + \frac{2Nk_o^{\max}}{(n_f - 1)nk_{\max}}. \quad (35)$$

We will show below that this choice also guarantees that the simulation samples the correct number of cyclisation and ligation events per unit volume and unit time as required by Eq. (6).

We define a *waiting time* variable that is set to zero at the beginning of the simulation. After each reaction, a waiting time increment is generated. These increments are also chosen in order to guarantee the correct number of ligation and fragmentation reactions per unit time/volume, as detailed below. We can now describe the MC step, during which the following actions are performed:

1. We evaluate the probability of annealing p according to Eq. (35). The explicit form of p, Eq. (35), will be discussed in detail below.

2. We pick a random number $0 \leq r \leq 1$ from a uniform distribution. If $r \leq p$, we attempt a ligation event:

    (a) We pick a pair of elements of the array $\mathbf{m}$, denoted α, β at random. Since there are $n_f(n_f - 1)$ ordered pairs of chains, the probability to pick a specific pair is $[n_f(n_f - 1)]^{-1}$. Let the length associated with these elements be $m_\alpha = i$ and $m_\beta = j$.

    (b) We evaluate the ligation rate $k_1(i,j)$ for the two chains. If $k_1(i,j) > k_{\max}$, we set $k_1^{\max} = k_1(i,j)$ and return to (1). Otherwise, we continue.

    (c) We pick another random number r', and perform the ligation if $r' \leq k_1(i,j)/k_1^{\max}$. If ligation is unsuccessful, we return to (1). Otherwise, we continue.

    (d) We increment the waiting time by $\Delta t_{i,j}^{\text{lig}} = \frac{2AN}{n_f(n_f-1)nk_{ij}}$. Here A is a parameter, the only condition on which is that it must be between 0 and 1, as we will discuss in more detail below.

    (e) After incrementing the waiting time, we update $\mathbf{f}$ by setting $m_\alpha = 0$ and $m_\beta = i + j$.

3. If $r > p$, we attempt a cyclisation event:

    (a) We pick a chain γ at random with probability n_f^{-1}. Let $m_\gamma = l$.

    (b) We evaluate the cyclisation rate $k_0(l)$. If $k_0(l) > k_0^{\max}$, set $k_0^{\max} = k_0(l)$ and return to (1). Otherwise, we continue.

    (c) We extract another random number $0 \leq r' \leq 1$ from a uniform distribution, and perform cyclisation if $r' \leq k_0(l)/k_0^{\max}$. If cyclisation is unsuccessful, we return to (1). Otherwise, we continue.

    (d) We increment the waiting time by $\Delta t_l^{\text{cyc}} = \frac{1-A}{n_f k_0(l)}$, with A defined above in step (2).

    (e) We record the value of l in $\mathbf{r}$ and set $m_\gamma = 0$.

We now prove that the definitions of p (Eq. (35)), the waiting time increments $\Delta t_{i,j}^{\text{lig}}$ (for ligation) and $\Delta t_{i,k-i}^{\text{cyc}}$ (for cyclisation) give a number of ligation and cyclisation events per unit time which is consistent with the Smoluchowski equation Eq. (6). Over a single MC step, the mean number of ligation events involving the ordered pair of filaments (α, β) is

$$\langle \#L_{\alpha,\beta} \rangle \equiv \frac{p}{n_f(n_f - 1)} \frac{k_1(m_\alpha, m_\beta)}{k_1^{\max}} . \qquad (36)$$

We note that in the algorithm we consider (m_α, m_β) as an ordered pair, and thus in (36) we consider the reaction

$(i,j) \to l$ as distinct from $(j,i) \to l$. The mean number of ligation events involving *any two chains* with lengths i, j can be obtained by multiplying the above quantity by $2(1 - \delta_{ij}/2)V^2 n_i n_j$. The factor $2(1 - \delta_{ij}/2)$ takes into account the fact that, as mentioned above, for $i \neq j$, there are two ways to perform the ligation, whereas for $i = j$ there is only one. The factor $V^2 n_i n_j$ is the product of the volume fractions of filaments of lengths i and j. We thus have

$$2V^2 n_i n_j \left(1 - \frac{\delta_{ij}}{2}\right) \times \frac{p}{n_f(n_f - 1)} \frac{k_1(i,j)}{k_1^{\max}} =$$
$$V k_1(i,j) n_i n_j \left(1 - \frac{\delta_{ij}}{2}\right) \Delta t , \qquad (37)$$

where we have equated the mean number of ligation events involving any two chains with lengths i, j to the value required by the Smoluchowski equation. Recalling that $n = N/V$, we thus find

$$\Delta t = \frac{2pN}{n_f(n_f - 1)nk_1^{\max}} . \qquad (38)$$

Eq. (38) relates the time interval Δt to the probability of ligation. We will now obtain a second equality involving p and Δt, which will allow us to prove that the expression Eq. (35) for p guarantees the correct number of ligation and cyclisation events per unit time.

The mean number of cyclisation events involving chains γ is

$$\langle \#C_\gamma \rangle \equiv \frac{(1-p)k_0(m_\gamma)}{n_f k_0^{\max}} . \qquad (39)$$

To obtain the mean number of cyclisations of a generic $l-$mer we need to multiply this quantity by $V n_l$, *i.e.*, the volume fraction of filaments of length l. Equating this quantity to the expected number of rings formed in a time interval Δt we obtain

$$V n_l \times \frac{(1-p)k_0(l)}{n_f k_0^{\max}} = k_0(l) n_l V \Delta t , \qquad (40)$$

and hence

$$\Delta t \equiv \frac{1-p}{n_f k_o^{\max}} . \qquad (41)$$

By equating the two expressions for Δt, Eq. (38) and Eq. (41), we find Eq. (35). We have thus proven that the latter is the correct expression of p, which gives the correct number of cyclisation and ligation events per unit time and unit volume, as required by the Smoluchowski equation.

Finally, we will prove below that the constants A and $1 - A$ introduced when calculating the waiting time increments are consistent with Eq. (38) and Eq. (41). To show this, it is sufficient to observe that the total time

increment during an MC step is:

$$\Delta t = \sum_{0 \leq \alpha < \beta \leq n_f - 1} \langle \#L_{\alpha,\beta} \rangle \Delta t^{\text{lig}}_{m_\alpha, m_\beta} + \sum_{i=1}^{m_\gamma - 1} \langle \#C_\gamma \rangle \Delta t^{\text{cyc}}_{m_\gamma}$$

$$= \sum_{0 \leq \alpha < \beta \leq n_f - 1} \left[\frac{p k_{m_\alpha, m_\beta}}{n_f(n_f - 1)k_{\max}} \right] \left[\frac{2AN}{n_f(n_f - 1)n k_{m_\alpha, m_\beta}} \right]$$

$$+ \sum_{i=1}^{m_\gamma - 1} \left[\frac{(1-p)k_o(l)}{n k_o^{\max}} \right] \frac{1 - A}{n_f k_o(l)}$$

$$= \frac{2ApN}{n_f(n_f - 1)n k_{\max}} + \frac{(1 - A)(1 - p)}{n_f k_o^{\max}}$$

$$(42)$$

One can see that this equality is consistent with Eq.(38) and Eq.(41). We note that the algorithm samples on average the correct kinetics independently of the value of A, as long as $0 \leq A \leq 1$. Here we take $A = 1$, meaning that the waiting time increment is calculated only after a successful ligation reaction, but not after a successful cyclisation reaction.

[1] K. Kremer and G. S. Grest, The Journal of Chemical Physics **92**, 5057 (1990).
[2] S. Plimpton, J. Comp. Phys. **117**, 1 (1995).
[3] R. M. Robertson, S. Laib, and D. E. Smith, Proc. Natl. Acad. Sci. USA **103**, 7310 (2006).
[4] W. H. Taylor and P. J. Hagerman, Journal of Molecular Biology **212**, 363 (1990).
[5] J. C. Crocker, M. T. Valentine, E. R. Weeks, T. Gisler, P. D. Kaplan, A. G. Yodh, and D. A. Weitz, Phys. Rev. Lett. **85**, 888 (2000).
[6] J.-P. Hansen and I. R. McDonald, *Theory of simple liquids: with applications to soft matter* (Academic press, 2013).
[7] P. G. De Gennes, The Journal of Chemical Physics **76**, 3316 (1982).
[8] J. Shimada and H. Yamakawa, Macromolecules **17**, 689 (1984).
[9] A. Rosa and R. Everaers, PLoS computational biology **4**, 1 (2008).
[10] M. Doi and S. Edwards, *The theory of polymer dynamics* (Oxford University Press, 1988).
[11] P. Meakin and M. H. Ernst, Phys. Rev. Lett. **60**, 2503 (1988).
[12] A. L. Garcia, C. Van Den Broeck, M. Aertsens, and R. Serneels, Physica A **143**, 535 (1987).
[13] K. Liffman, J. Comput. Phys. **100**, 116 (1992).
[14] F. E. Kruis, A. Maisels, and H. Fissan, AIChE J. **46**, 1735 (2000).